Experimental Investigation of a Path Following Controller for Planar Snake Robots

Pål Liljebäck[1,2], Idar U. Haugstuen[1], Kristin Y. Pettersen[1]
[1]Norwegian University of Science and Technology, Dept. of Engineering Cybernetics, NO-7491 Trondheim, Norway
[2]SINTEF ICT, Dept. of Applied Cybernetics, N-7465 Trondheim, Norway
E-mail addresses: Pal.Liljeback@sintef.no, haugstue@stud.ntnu.no, Kristin.Y.Pettersen@itk.ntnu.no

***Abstract*—This paper considers path following control of snake robots along straight paths. A controller is proposed which, under the assumption that the forward velocity of the snake robot is nonzero and positive, guarantees $\mathcal{K}$-exponential stability of the distance between the snake robot and the desired path and also $\mathcal{K}$-exponential stability of the heading of the robot with respect to the direction of the path. The performance of the path following controller is investigated through experiments with a physical snake robot. The experiments show that the proposed controller successfully steers the snake robot towards and along the desired straight path.**

***Index Terms*—Snake robot, Path following, Cascaded systems, K-exponential stability.**

I. Introduction

Inspired by biological snakes, snake robots carry the potential of meeting the growing need for robotic mobility in challenging environments. Snake robots consist of serially connected modules capable of bending in one or more planes. The many degrees of freedom of snake robots make them difficult to control, but provide traversability in irregular environments that surpasses the mobility of the more conventional wheeled, tracked and legged forms of robotic mobility.

This paper considers planar path following control of snake robots along straight paths. Straight line path following capabilities are important since they enable a snake robot to follow a desired path given by waypoints interconnected by straight lines. Straight line path following is therefore relevant for many future applications of snake robots, such as automated inspection rounds in inaccessible areas of industrial process facilities or mapping of confined spaces by moving along prescribed paths. Note that this paper considers path following, in contrast to trajectory tracking, where the goal is additionally to control the position of the system *along* the path. During path following, we steer the system towards and along the path, but do not consider the position of the system along the path.

Research on snake locomotion has been conducted for several decades. Gray [1] conducted empirical and analytical studies of snake locomotion already in the 1940s, and Hirose [2] studied biological snakes and developed mathematical relationships characterizing their motion, such as the *serpenoid curve*. The main emphasis in literature so far has mainly been on achieving forward and turning locomotion. The next step will be not only to achieve locomotion, but also to make the snake robot follow a desired path. The research on this control problem is still limited. The work in [3] considers trajectory tracking of snake robots where a number of the links are assumed to be wheeled (no-slip constraints) so that the underactuation of the system is removed. Path following of a snake robot with active wheels is considered in [4], but no stability analysis of the controller is presented. The authors have previously employed *Poincaré maps* to study the stability properties of snake locomotion along a straight path [5]. The presented analysis is, however, based on numerical calculations and is thus only valid for a given set of controller parameters.

Research on robotic fish and eel-like mechanisms is relevant to research on snake robots since these mechanisms are very similar. The works in [6]–[8] synthesize gaits for translational and rotational motion of various fish-like mechanisms and propose controllers for tracking straight and curved trajectories. However, an analysis that formally proves that the fish-like mechanisms converge to the desired path still remains.

In this paper, we consider the problem of planar path following control of snake robots. The contribution is an experimental investigation of a path following controller proposed by the authors in [9] that enables snake robots to track a planar straight path. Under the assumption that the forward velocity of the snake robot is nonzero and positive, the proposed controller guarantees $\mathcal{K}$-exponential stability of the distance between the snake robot and the desired path and also $\mathcal{K}$-exponential stability of the heading of the robot with respect to the direction of the path. The performance of the path following controller is investigated through experiments with a physical snake robot. The experiments show that the proposed controller successfully steers the snake robot towards and along the desired straight path.

The paper is organized as follows. Section II presents the model of the snake robot. Section III presents the path following controller. Section IV describes the setup employed in order to experimentally investigate the path following controller. Section V presents the experimental results. Finally, Section VI presents concluding remarks.

II. The model of the snake robot

This section summarizes the model of the snake robot which the controller development in Section III is based upon. For a more detailed presentation of the model, the reader is referred to [10].

A. Overview of the model

We consider a planar snake robot with links interconnected by active revolute joints. The surface beneath the robot is flat and horizontal, and each link is subjected to a viscous ground friction force. The body shape changes of the robot induce friction forces on the links that produce the translational and rotational motion of the robot. A simplified model that captures

978-1-4244-7815-6/10/$26.00

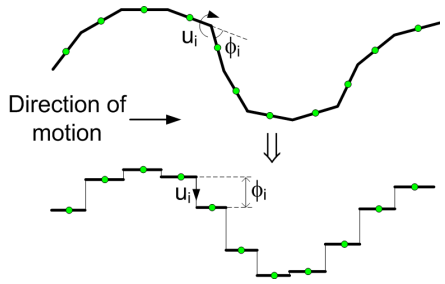

Fig. 1. The revolute joints of the snake robot are modelled as prismatic joints that displace the CM of each link transversal to the direction of motion.

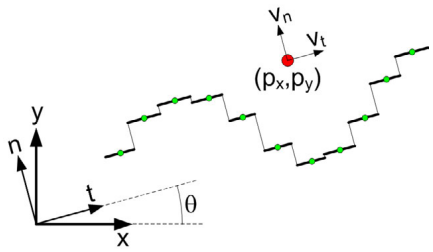

Fig. 2. Illustration of the two coordinate frames employed in the model. The global x-y frame is fixed. The t-n frame is always aligned with the snake robot.

only the most essential part of the snake robot dynamics is proposed in [10]. The idea behind this model is illustrated in Fig. 1 and motivated by an analysis presented in [10], which shows that:

- The forward motion of a planar snake robot is produced by the link velocity components that are *normal* to the forward direction.
- The change in body shape during forward locomotion primarily consists of relative displacements of the CM of the links *normal* to the forward direction of motion.

Based on these two properties, the simplified model describes the body shape changes of a snake robot as *linear displacements* of the links with respect to each other instead of rotational displacements. The linear displacements occur *normal* to the forward direction of motion and produce friction forces that propel the robot forward. This essentially means that the revolute joints of the snake robot are modelled as prismatic (translational) joints and that the rotational motion of the links during body shape changes is disregarded. However, the model still captures the *effect* of the rotational link motion during body shape changes, which is a linear displacement of the CM of the links normal to the forward direction of motion.

The mathematical model of the snake robot is summarized in the next subsection in terms of the symbols illustrated in Fig. 2 and Fig. 3.

B. Equations of motion

The snake robot has N links of length l and mass m interconnected by $N-1$ prismatic joints. The prismatic joints control the normal direction distance between the links. As seen in Fig. 3, the normal direction distance from link i to

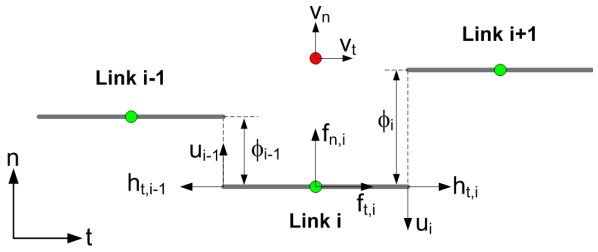

Fig. 3. Symbols characterizing the kinematics and dynamics of the snake robot.

link $i+1$ is denoted by ϕ_i and represents the coordinate of joint i. The positive direction of ϕ_i is along the n axis.

The snake robot moves in the horizontal plane and has $N+2$ degrees of freedom. The motion is defined with respect to the two coordinate frames illustrated in Fig. 2. The x-y frame is the fixed global frame. The t-n frame is always aligned with the snake robot, i.e. the t and n axis always point in the *tangential* and *normal* direction of the robot, respectively. The origin of both frames coincide.

As seen in Fig. 2, the global frame position of the CM (center of mass) of the snake robot is denoted by $(p_x, p_y) \in \mathbb{R}^2$. The global frame orientation, denoted by $\theta \in \mathbb{R}$, is defined as the angle between the t axis and the global x axis with counterclockwise positive direction.

The state vector of the system is chosen as

$$\boldsymbol{x} = (\boldsymbol{\phi}, \theta, p_x, p_y, \boldsymbol{v}_\phi, v_\theta, v_t, v_n) \in \mathbb{R}^{2N+4} \tag{1}$$

where $\boldsymbol{\phi} = (\phi_1, \cdots, \phi_{N-1}) \in \mathbb{R}^{N-1}$ are the joint coordinates, $\theta \in \mathbb{R}$ is the absolute orientation, $(p_x, p_y) \in \mathbb{R}^2$ is the global frame position of the CM, $\boldsymbol{v}_\phi = \dot{\boldsymbol{\phi}} \in \mathbb{R}^{N-1}$ are the joint velocities, $v_\theta = \dot{\theta} \in \mathbb{R}$ is the angular velocity, and $(v_t, v_n) \in \mathbb{R}^2$ is the tangential and normal direction velocity of the snake robot. Note that we define the position with respect to the global frame, but the translational velocity with respect to the t-n frame.

As illustrated in Fig. 3, each link is influenced by a ground friction force (acting on the CM of the link) and constraint forces that hold the joints together. A model of these forces is presented in [10], where it is also shown that the complete model of the snake robot can be written as

$$\dot{\boldsymbol{\phi}} = \boldsymbol{v}_\phi \tag{2a}$$
$$\dot{\theta} = v_\theta \tag{2b}$$
$$\dot{p}_x = v_t \cos\theta - v_n \sin\theta \tag{2c}$$
$$\dot{p}_y = v_t \sin\theta + v_n \cos\theta \tag{2d}$$
$$\dot{\boldsymbol{v}}_\phi = -\frac{c_1}{m}\boldsymbol{v}_\phi + \frac{c_2}{m} v_t \boldsymbol{A}\boldsymbol{D}^T\boldsymbol{\phi} + \frac{1}{m}\boldsymbol{D}\boldsymbol{D}^T\boldsymbol{u} \tag{2e}$$
$$\dot{v}_\theta = -c_3 v_\theta + \frac{c_4}{N-1} v_t \overline{\boldsymbol{e}}^T\boldsymbol{\phi} \tag{2f}$$
$$\dot{v}_t = -\frac{c_1}{m} v_t + \frac{2c_2}{Nm} v_n \overline{\boldsymbol{e}}^T\boldsymbol{\phi} - \frac{c_2}{Nm}\boldsymbol{\phi}^T\boldsymbol{A}\overline{\boldsymbol{D}}\boldsymbol{v}_\phi \tag{2g}$$
$$\dot{v}_n = -\frac{c_1}{m} v_n + \frac{2c_2}{Nm} v_t \overline{\boldsymbol{e}}^T\boldsymbol{\phi} \tag{2h}$$

where $\boldsymbol{u} \in \mathbb{R}^{N-1}$ are the actuator forces at the joints and $\overline{\boldsymbol{e}} = \begin{bmatrix} 1 & . & . & 1 \end{bmatrix}^T \in \mathbb{R}^{N-1}$,

$$\overline{\boldsymbol{D}} = \boldsymbol{D}^T \left(\boldsymbol{D}\boldsymbol{D}^T\right)^{-1} \in \mathbb{R}^{N\times(N-1)},$$

$$\boldsymbol{A} = \begin{bmatrix} 1 & 1 & & \\ & \cdot & \cdot & \\ & & \cdot & \cdot \\ & & 1 & 1 \end{bmatrix}, \boldsymbol{D} = \begin{bmatrix} 1 & -1 & & \\ & \cdot & \cdot & \\ & & \cdot & \cdot \\ & & 1 & -1 \end{bmatrix},$$

where $\boldsymbol{A} \in \mathbb{R}^{(N-1)\times N}$ and $\boldsymbol{D} \in \mathbb{R}^{(N-1)\times N}$. The parameters c_1, c_2, c_3, and c_4 are scalar friction coefficients that characterize the external forces acting on the snake robot. In particular, the coefficient c_1 determines the magnitude of the friction forces resisting the link motion, c_2 determines the magnitude of the induced friction forces that propel the snake robot forward, c_3 determines the friction torque opposing the rotation of the snake robot, while c_4 determines the induced torque that rotates the snake robot. This torque is induced when the forward direction velocity and the average of the joint coordinates are nonzero. The role of each coefficient is explained in more detail in [10].

III. Design of the path following controller

This section presents the straight line path following controller for the snake robot.

A. Control objective

The control objective is to steer the snake robot so that it converges to and subsequently tracks a straight path while maintaining a heading which is parallell to the path. To this end, we define the global coordinate system so that the global x axis is aligned with the desired straight path. The position of the snake robot along the global y axis, p_y, is thereby the shortest distance from the robot to the desired path and the orientation of the snake robot, θ, is the angle that the robot forms with the desired path. The control objective is thereby to regulate p_y and θ to zero. Since snake robot locomotion is a slow form of robotic mobility which is generally employed for traversability purposes, the authors consider it less important to accurately control the forward velocity of the robot. During path following with a snake robot, it therefore makes sense to focus all the control efforts on converging to the path and subsequently progressing along the path at some nonzero forward velocity $v_t \in [V_{\min}, V_{\max}]$, where $V_{\min}$ and $V_{\max}$ represent the boundaries of some positive interval containing the forward velocity.

From the above discussion, the control problem is to design a (possibly time-varying) feedback control law

$$\boldsymbol{u} = \boldsymbol{u}(t, \boldsymbol{\phi}, \theta, p_y, \boldsymbol{v}_\phi, v_\theta, v_t, v_n) \in \mathbb{R}^{N-1} \tag{3}$$

such that the following control objectives are reached:

$$\lim_{t\to\infty} \; p_y(t) = 0 \tag{4}$$

$$\lim_{t\to\infty} \; \theta(t) = 0 \tag{5}$$

B. Assumptions

A planar snake robot achieves forward motion through periodic body shape changes that generate external forces on the robot from the environment, which propel the robot forward. The most common form of such periodic body shape changes is called *lateral undulation* [2] and consists of horizontal waves that are propagated backwards along the snake body from head to tail. The work by the authors in [11], which investigates the velocity dynamics of a snake robot during lateral undulation, shows that the forward velocity during lateral undulation oscillates around a positive nonzero average velocity that can be predetermined based on the parameters characterizing the gait pattern. In other words, when the snake robot conducts lateral undulation, the results in [11] suggest that the forward velocity is contained in some nonzero and positive interval $[V_{\min}, V_{\max}]$ that can be scaled based on a set of gait pattern parameters. We therefore choose to base the path following controller of the snake robot on the following assumption:

Assumption 1: The snake robot conducts *lateral undulation* and has a forward velocity which is always nonzero and positive, i.e. $v_t \in [V_{\min}, V_{\max}] \; \forall \; t \geq 0$ where $V_{\max} \geq V_{\min} > 0$.

C. Model transformation

On the basis of Assumption 1, we will disregard the dynamics of the forward velocity v_t given by (2g) and instead treat the forward velocity as a positive parameter satisfying $v_t \in [V_{\min}, V_{\max}]$.

As seen in (2f) and (2h), the joint coordinates $\boldsymbol{\phi}$ are present in the dynamics of both the angular velocity v_θ and the sideways velocity v_n of the snake robot. This complicates the controller design since the body shape changes will affect both the heading and the sideways motion of the robot. Motivated by [12], we therefore remove the effect of $\boldsymbol{\phi}$ on the sideways velocity by the coordinate transformation:

$$\overline{p}_x = p_x + \epsilon \cos\theta \tag{6a}$$

$$\overline{p}_y = p_y + \epsilon \sin\theta \tag{6b}$$

$$\overline{v}_n = v_n + \epsilon v_\theta \tag{6c}$$

where ϵ is a constant parameter defined as

$$\epsilon = -\frac{2\,(N-1)}{Nm}\frac{c_2}{c_4} \tag{7}$$

The new coordinates in (6) transforms the model (2) into

$$\dot{\boldsymbol{\phi}} = \boldsymbol{v}_\phi \tag{8a}$$

$$\dot{\theta} = v_\theta \tag{8b}$$

$$\dot{\overline{p}}_x = v_t \cos\theta - \overline{v}_n \sin\theta \tag{8c}$$

$$\dot{\overline{p}}_y = v_t \sin\theta + \overline{v}_n \cos\theta \tag{8d}$$

$$\dot{\boldsymbol{v}}_\phi = -\frac{c_1}{m}\boldsymbol{v}_\phi + \frac{c_2}{m} v_t \boldsymbol{A}\boldsymbol{D}^T\boldsymbol{\phi} + \frac{1}{m}\boldsymbol{D}\boldsymbol{D}^T\boldsymbol{u} \tag{8e}$$

$$\dot{v}_\theta = -c_3 v_\theta + \frac{c_4}{N-1} v_t \overline{\boldsymbol{e}}^T\boldsymbol{\phi} \tag{8f}$$

$$\dot{\overline{v}}_n = X v_\theta + Y \overline{v}_n \tag{8g}$$

where, by Assumption 1, the parameter $v_t \in [V_{\min}, V_{\max}]$ and $V_{\max} \geq V_{\min} > 0$, and where

$$X = \epsilon\left(\tfrac{c_1}{m} - c_3\right), \quad Y = -\tfrac{c_1}{m} \tag{9}$$

The two scalar constants X and Y have been introduced in (8g) for simplicity of notation in the following sections.

Remark 2: The coordinate transformation (6) is illustrated to the left in Fig. 4 and can be interpreted as moving the point that determines the position of the snake robot a distance ϵ

along the tangential direction of the robot to a new location, which is precisely where the body shape changes of the robot (characterized by $\overline{\boldsymbol{e}}^T\boldsymbol{\phi}$) generate a pure rotational motion and no sideways force.

D. The path following controller

The path following controller of the snake robot consists of two main components. The first component is the gait pattern controller, which propels the snake robot forward according to the gait pattern *lateral undulation* (as stated in Assumption 1). The second component is the heading controller, which steers the snake robot towards and subsequently along the desired path. The two components of the path following controller are now presented.

1) Gait pattern controller: As proposed in [2], lateral undulation is achieved by controlling joint $i \in \{1, \cdots, N-1\}$ of the snake robot according to the sinusoidal reference

$$\phi_{i,\text{ref}} = \alpha \sin\left(\omega t + (i-1)\,\delta\right) + \phi_o \tag{10}$$

where α and ω are the amplitude and frequency, respectively, of the sinusoidal joint motion and δ determines the phase shift between the joints. The parameter ϕ_o is a joint offset coordinate that we will use to control the direction of the locomotion. In order to make the joints track the joint reference coordinates given by (10), we set the actuator forces according to the linearizing control law

$$\boldsymbol{u} = m\left(\boldsymbol{D}\boldsymbol{D}^T\right)^{-1}\left(\overline{\boldsymbol{u}} + \frac{c_1}{m}\dot{\boldsymbol{\phi}} - \frac{c_2}{m}v_t\boldsymbol{A}\boldsymbol{D}^T\boldsymbol{\phi}\right) \tag{11}$$

where $\overline{\boldsymbol{u}} \in \mathbb{R}^{N-1}$ is a new set of control inputs. This control law transforms the joint dynamics (8e) into $\dot{\boldsymbol{v}}_\phi = \ddot{\boldsymbol{\phi}} = \overline{\boldsymbol{u}}$. Subsequently, we choose the new control input $\overline{\boldsymbol{u}}$ as

$$\overline{\boldsymbol{u}} = \ddot{\boldsymbol{\phi}}_{\text{ref}} + k_{v_\phi}\left(\dot{\boldsymbol{\phi}}_{\text{ref}} - \dot{\boldsymbol{\phi}}\right) + k_\phi\left(\boldsymbol{\phi}_{\text{ref}} - \boldsymbol{\phi}\right) \tag{12}$$

where $k_\phi > 0$ and $k_{v_\phi} > 0$ are scalar controller gains and $\boldsymbol{\phi}_{\text{ref}} = (\phi_{1,\text{ref}}, \cdots, \phi_{N-1,\text{ref}}) \in \mathbb{R}^{N-1}$ are the joint reference coordinates given by (10). By introducing the error variable $\widetilde{\boldsymbol{\phi}} = \boldsymbol{\phi} - \boldsymbol{\phi}_{\text{ref}}$, the resulting error dynamics of the joints can be written as

$$\ddot{\widetilde{\boldsymbol{\phi}}} + k_{v_\phi}\dot{\widetilde{\boldsymbol{\phi}}} + k_\phi\widetilde{\boldsymbol{\phi}} = 0 \tag{13}$$

which is clearly *exponentially stable* [13].

2) Heading controller: In order to steer the snake robot towards the desired straight path, we employ the Line-of-Sight (LOS) guidance law

$$\theta_{\text{ref}} = -\arctan(\frac{\overline{p}_y}{\Delta}) \tag{14}$$

where $\overline{p}_y$ is the cross-track error and $\Delta > 0$ is a design parameter referred to as the *look-ahead distance*. This LOS guidance law is commonly used during e.g. path following control of marine surface vessels [12], [14]. As illustrated to the right in Fig. 4, the LOS angle θ_{ref} corresponds to the orientation of the snake robot when it is headed towards the point located a distance Δ ahead of the snake robot along the desired path. The value of Δ is important since it will determine the rate of convergence to the desired path.

As mentioned in Section III-D1, we will use the joint offset coordinate ϕ_o in (10) to ensure that the heading of

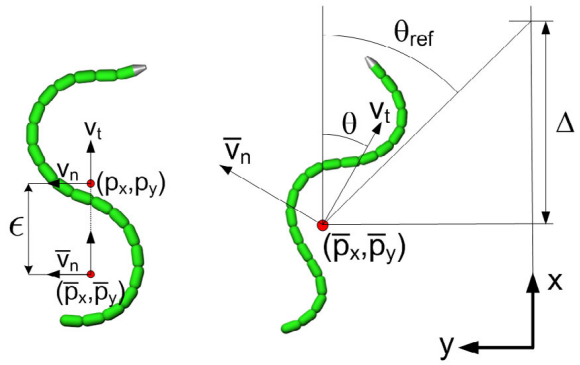

Fig. 4. Left: The coordinate transformation of the snake robot. Right: The Line-of-Sight (LOS) guidance system.

the snake robot θ tracks the LOS angle given by (14). To derive the control law for ϕ_o, we first use (10) and the relation $\boldsymbol{\phi} = \boldsymbol{\phi}_{\text{ref}} + \widetilde{\boldsymbol{\phi}}$ in order to rewrite (8f) as

$$\begin{aligned}\dot{v}_\theta = -c_3 v_\theta + c_4 v_t \phi_o \\ + \tfrac{c_4}{N-1} v_t \left(\sum_{i=1}^{N-1} \alpha \sin(\omega t + (i-1)\,\delta) + \overline{\boldsymbol{e}}^T\widetilde{\boldsymbol{\phi}}\right)\end{aligned} \tag{15}$$

Consequently, choosing ϕ_o as

$$\begin{aligned}\phi_o = \tfrac{1}{c_4 v_t}\Big(\ddot{\theta}_{\text{ref}} + c_3\dot{\theta}_{\text{ref}} - k_\theta(\theta - \theta_{\text{ref}}) \\ - \tfrac{c_4}{N-1} v_t \sum_{i=1}^{N-1} \alpha \sin(\omega t + (i-1)\,\delta)\Big)\end{aligned} \tag{16}$$

where $k_\theta > 0$ is a scalar controller gain, enables us to write the error dynamics of the heading angle θ as

$$\ddot{\widetilde{\theta}} + c_3\dot{\widetilde{\theta}} + k_\theta\widetilde{\theta} = \frac{c_4}{N-1} v_t \overline{\boldsymbol{e}}^T\widetilde{\boldsymbol{\phi}} \tag{17}$$

where we have introduced the error variable $\widetilde{\theta} = \theta - \theta_{\text{ref}}$. The error dynamics of the joints in (13) and of the heading in (17) represent a cascaded system. In particular, the system (13) perturbs the system (17) through the interconnection term $\frac{c_4}{N-1} v_t \overline{\boldsymbol{e}}^T\widetilde{\boldsymbol{\phi}}$. It is shown in [9] that the origin of this cascaded system is globally $\mathcal{K}$-exponentially stable.

Remark 3: The joint angle offset in (16) depends on the inverse of the forward velocity. This does not represent a problem since $v_t > 0$ by Assumption 1. When implementing the path following controller, this issue can be avoided by activating the controller *after* the snake robot has obtained a positive forward velocity.

We have now presented the complete path following controller of the snake robot, whose structure is summarized in Fig. 5. The controller satisfies the following theorem:

Theorem 4: Consider a planar snake robot described by the model (8) and suppose that Assumption 1 is satisfied. If the parameter Δ of the LOS guidance law (14) is chosen such that

$$\Delta > \frac{|X|}{|Y|}\left(1 + \frac{V_{\max}}{V_{\min}}\right) \tag{18}$$

then the path following controller defined by (10), (11), (12), (14), and (16) guarantees that the control objectives (4) and (5) are achieved for any set of initial conditions satisfying $v_t \in [V_{\min}, V_{\max}]$.

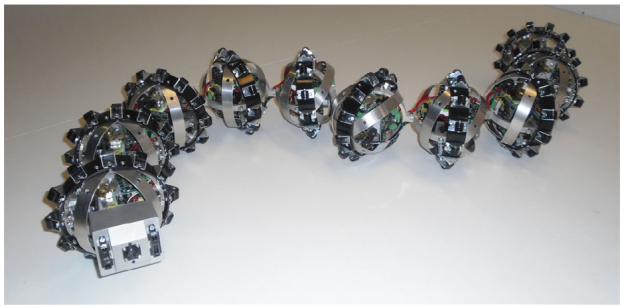

Fig. 6. The snake robot used in the experiment.

TABLE I
PARAMETERS OF A JOINT MODULE.

Parameter	Value
Total weight of a joint module	960 g
Outer diameter	130 mm
Degrees of freedom	2
Max joint travel	$\pm 45°$
Max continuous joint torque	4.5 Nm
Max joint speed (no load)	$70°/\text{sec}$

Proof: The proof of this theorem is presented in [9] and is not included here due to space restrictions. ■

Remark 5: Theorem 4 does not specify the boundary values $V_{\min}$ and $V_{\max}$ of the interval in which the forward velocity v_t is contained. By Assumption 1, however, there exists a positive interval that contains v_t for all time $t \geq 0$. Specifying $V_{\min}$ and $V_{\max}$ as a function of the gait pattern parameters α, ω, δ, and ϕ_o remains a topic of future work.

IV. EXPERIMENTAL SETUP

This section describes the experimental setup employed in order to investigate the performance of the path following controller proposed in the previous section.

A. The snake robot

The snake robot used in the experiments is shown in Fig. 6. A detailed description of the internal components of the robot is given in [15]. The snake robot consists of 10 identical joint modules characterized by the parameters listed in Table I. Each joint module has 2 degrees of freedom (pitch and yaw motion) driven by two Hitec servo motors (HS-5955TG). The pitch and yaw angle of the joint modules are measured with magnetic rotary encoders (AS5043 from austriamicrosystems).

As shown to the left in Fig. 8, each joint module is covered by 12 small wheels. These wheels ensure that the ground friction forces acting on the snake robot are *anisotropic*, i.e. that the friction coefficient characterizing the ground friction forces in the normal (sideways) direction of each joint is larger than the tangential (forward) direction friction coefficient. This property is essential for efficient snake locomotion on a planar surface and is also present in the model of the snake robot (2).

Each joint module is battery-powered and contains a custom-designed microcontroller card used to control the joint angles. A microcontroller card (the brain card) located in the head of the snake robot transmits joint reference angles to all joint modules over a CAN bus running through the robot. The joint reference angles are calculated on an external computer and sent to the brain card via a wireless connection based on Bluetooth. The refresh rate for the two reference angles of each joint module is about 20 Hz.

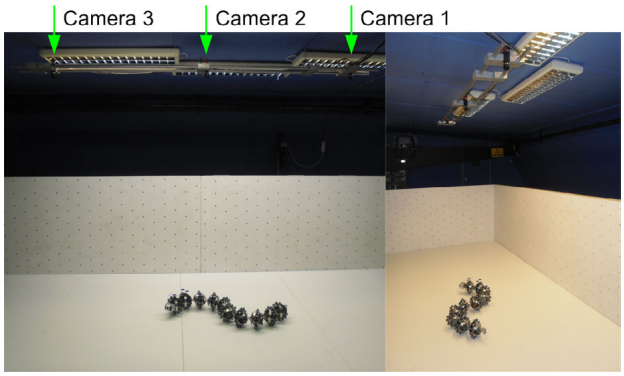

Fig. 7. The experimental setup. Three cameras mounted in the ceiling measured the position of the snake robot on a horizontal surface measuring about 240 cm in width and 600 cm in length.

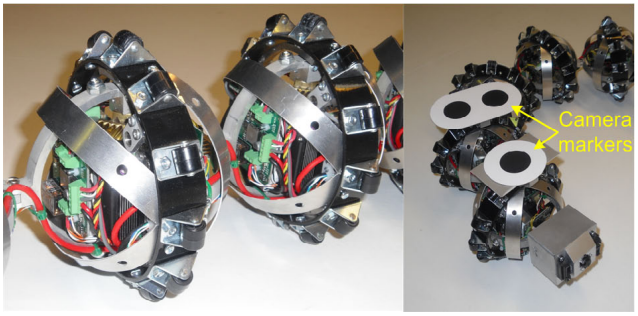

Fig. 8. Left: The wheels installed around each joint module in order to give the robot anisotropic ground friction properties. Right: The black markers mounted on the snake robot to allow the position to be tracked by SwisTrack.

B. The camera-based position measurement system

During the experiments, the snake robot moved on a white horizontal surface measuring about 240 cm in width and 600 cm in length. This is shown in Fig. 7. The 2D position of the robot was measured by use of the open source camera tracking software *SwisTrack* [16]. SwisTrack was configured to read camera data at 15 frames per second from three firewire cameras (Unibrain Fire-i 520c) mounted in the ceiling above the snake robot as shown in Fig. 7. The use of multiple cameras allowed for position measurements over a greater distance than the area covered by a single camera. The cameras were mounted facing downwards approximately 218 cm above the floor and 132 cm apart.

SwisTrack was configured to track black circular markers (40 mm in diameter) mounted on the snake robot as shown to the right in Fig. 8. The conversion from the pixel position of a marker to the real-world position (in cm) was conducted by SwisTrack based on a specific calibration method available in this software. SwisTrack estimated the maximum position error to be about 1.9 cm and the average position error to be about 0.6 cm. The global frame position, x_{head} and y_{head}, and the angle, θ_{head}, of the head of the snake robot was calculated

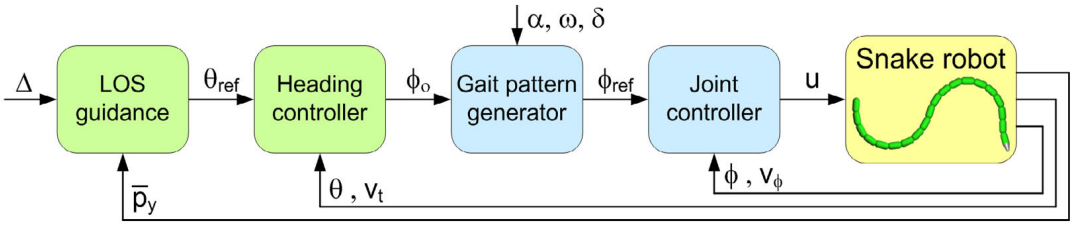

Fig. 5. The structure of the path following controller.

from the individual marker positions. Knowing the position and orientation of the head, and also the individual joint angles, we employed simple kinematic relationships presented in [17] in order to calculate the position of the center of mass, p_x and p_y, of the snake robot. Furthermore, we estimated the orientation, θ, of the robot as the average of the individual absolute link angles.

C. Implementation of the path following controller

The controller was implemented on an external computer according to (10), (14), and (16). We did not implement the joint torque controller given by (11) and (12) since accurate torque control is not supported by the servo motors installed in the snake robot. The joint angles were therefore controlled according to a proportional controller implemented in the microcontroller of each joint module.

The coordinate transformation distance ϵ defined in (7) was assumed to be negligible, i.e. we assumed that the sideways motion of the CM of the snake robot is zero during turning locomotion, which is a reasonable approximation. This means that $\overline{p}_y = p_y$ during the experiment.

The LOS angle θ_{ref} given by (14) was calculated with a look-ahead distance Δ equal to the length of the snake robot, i.e. $\Delta = 1.4$ m. We conjecture, but cannot prove, that this value is well above the lower limit of Δ given by (18). As noted in Remark 5, specifying Δ as a function of the gait pattern parameters α, ω, δ, and ϕ_o remains a topic of future work. To ensure a smooth control input, the LOS angle θ_{ref} was passed through a 3rd order low-pass filtering reference model (see e.g. Chapter 5 in [14]). The output from this filter also provided the derivatives of θ_{ref} with respect to time, which are required in the calculation of ϕ_o in (16). The evolution of the reference values from the filter were calculated with a first-order numerical integration scheme.

The forward velocity v_t of the robot, which is needed in (16), was estimated at 0.5 Hz as the displacement of the CM of the robot divided by the sampling interval (i.e. 2 s). The large sampling interval was necessary to avoid large variations in the velocity estimate, but was sufficient since the robot was moved at a slow pace during the experiment.

The joint angle offset ϕ_o given by (16) was calculated with the gains set to $k_\theta = 0.7$, $c_3 = 0.5$ and $c_4 = 20$. Note that c_3 and c_4 are actually friction coefficients in the model (2). It is not clear, however, how these values should be set in order to reflect the specific friction conditions during the experiment. We therefore chose these parameters in accordance with the parameters used during a simulation study in [10], where the model (2) was shown to compare well with a more complex model of snake robot locomotion. The joint angle offset was saturated according to $\phi_o \in [-25°, 25°]$ in order to keep the joint reference angles within reasonable bounds with respect to the maximum allowable joint angles of the physical snake robot. This saturation also avoided the singularity in (16) at $v_t = 0$ (see Remark 3). Furthermore, we restricted ϕ_o from changing faster than $\pm 10°$/s to enforce a smooth motion of the snake robot.

The reference angles corresponding to the horizontal joint motion of the robot were calculated according to (10) with $N = 10$ links and with gait parameters set to $\alpha = 30°$, $\omega = 50°$/s, and $\delta = 36°$. The reference angles corresponding to the vertical joint motion were set to zero to achieve a purely planar locomotion.

V. Experimental results

The proposed path following controller was experimentally investigated from two different sets of initial conditions. In the first trial of the experiment, the initial state of the snake robot was approximately $\boldsymbol{\phi} = \mathbf{0}°$, $\theta = 90°$, $p_x = 0.5$ m, $p_y = 0.5$ m, $\boldsymbol{v}_\phi = \mathbf{0}°/\text{s}$, $v_\theta = 0°/\text{s}$, $v_t = 0$ m/s, and $v_n = 0$ m/s, i.e. the snake robot was initially headed away from the desired path (the x axis) and the initial distance from the CM to the desired path was 0.5 m. In the second trial, the initial state of the robot was approximately $\boldsymbol{\phi} = \mathbf{0}°$, $\theta = -90°$, $p_x = 0.4$ m, $p_y = 1$ m, $\boldsymbol{v}_\phi = \mathbf{0}°/\text{s}$, $v_\theta = 0°/\text{s}$, $v_t = 0$ m/s, and $v_n = 0$ m/s, i.e. the snake robot was initially headed towards the desired path (the x axis) and the initial distance from the CM to the desired path was 1 m.

The motion of the snake robot during the first trial is shown in Fig. 9 and Fig. 10, while the motion during the second trial is shown in Fig. 11. The black line on the floor in the pictures of Fig. 9 indicates the desired path, i.e. the global x axis. The pictures show that the robot converges nicely towards and along the desired path. This is supported by the measurements in Fig. 10 and Fig. 11, which show that the cross-track error p_y and the orientation θ converge towards and subsequently oscillate around zero from both initial conditions. The plots also show the measured joint angles of an arbitrarily chosen joint (joint 5) during the path following, which indicate a very good tracking of the joint reference angles. In summary, the experiment showed that the proposed controller successfully steers the snake robot towards and along the desired straight path.

VI. Conclusions and future work

This paper has proposed a path following controller that enables snake robots to track straight paths. A controller has been proposed which, under the assumption that the forward velocity of the snake robot is nonzero and positive, guarantees

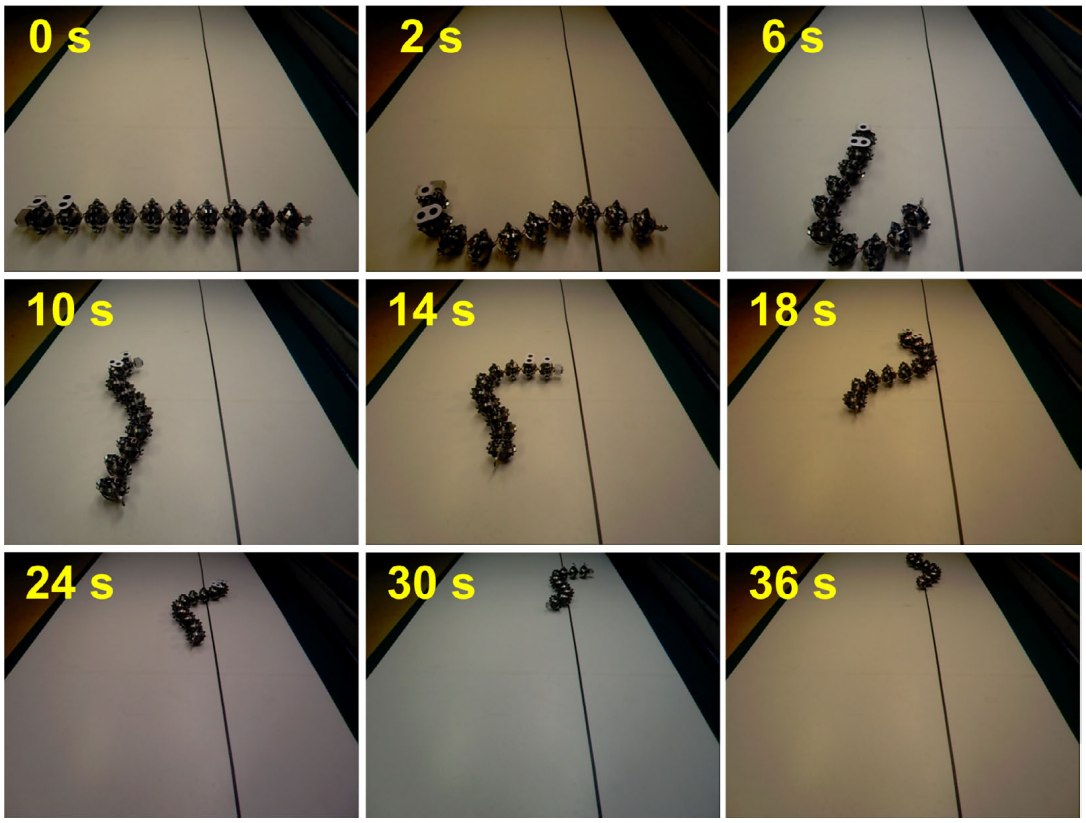

Fig. 9. The motion of the snake robot during path following with an initial heading away from the desired path. The black line on the floor indicates the desired path, i.e. the global x axis.

$\mathcal{K}$-exponential stability of the distance between the snake robot and the desired path and also $\mathcal{K}$-exponential stability of the heading of the robot with respect to the direction of the path. The performance of the path following controller was investigated through experiments with a physical snake robot. During the experiments, the proposed controller successfully steered the snake robot towards and along the desired straight path. In future work, the authors will specify the bounds on the forward velocity of the snake robot in terms of the gait pattern parameters.

REFERENCES

[1] J. Gray, "The mechanism of locomotion in snakes," *J. Exp. Biol.*, vol. 23, no. 2, pp. 101–120, 1946.

[2] S. Hirose, *Biologically Inspired Robots: Snake-Like Locomotors and Manipulators*. Oxford: Oxford University Press, 1993.

[3] F. Matsuno and H. Sato, "Trajectory tracking control of snake robots based on dynamic model," in *Proc. IEEE Int. Conf. on Robotics and Automation*, 2005, pp. 3029–3034.

[4] B. Murugendran, A. A. Transeth, and S. A. Fjerdingen, "Modeling and path-following for a snake robot with active wheels," in *Proc. IEEE/RSJ Int. Conf. Intelligent Robots and Systems*, 2009, pp. 3643 – 3650.

[5] P. Liljebäck, K. Y. Pettersen, Ø. Stavdahl, and J. T. Gravdahl, "Stability analysis of snake robot locomotion based on poincaré maps," in *Proc. IEEE/RSJ Int. Conf. Intelligent Robots and Systems*, 2009, pp. 3623–3630.

[6] P. A. Vela, K. A. Morgansen, and J. W. Burdick, "Underwater locomotion from oscillatory shape deformations," in *Proc. IEEE Conf. Decision and Control*, vol. 2, Dec. 2002, pp. 2074–2080 vol.2.

[7] K. McIsaac and J. Ostrowski, "Motion planning for anguilliform locomotion," *IEEE Trans. Robot. Autom.*, vol. 19, no. 4, pp. 637–625, August 2003.

[8] K. Morgansen, B. Triplett, and D. Klein, "Geometric methods for modeling and control of free-swimming fin-actuated underwater vehicles," *IEEE Transactions on Robotics*, vol. 23, no. 6, pp. 1184–1199, Dec 2007.

[9] P. Liljebäck, I. U. Haugstuen, and K. Y. Pettersen, "Path following control of planar snake robots using a cascaded approach," in *Proc. IEEE Int. Conf. Decision and Control*, 2010, accepted.

[10] P. Liljebäck, K. Y. Pettersen, Ø. Stavdahl, and J. T. Gravdahl, "A simplified model of planar snake robot locomotion," in *Proc. IEEE/RSJ Int. Conf. Intelligent Robots and Systems*, 2010, accepted.

[11] ——, "Stability analysis of snake robot locomotion based on averaging theory," in *Proc. IEEE Int. Conf. Decision and Control*, 2010, accepted.

[12] E. Fredriksen and K. Y. Pettersen, "Global κ-exponential way-point maneuvering of ships: Theory and experiments," *Automatica*, vol. 42, pp. 677 – 687, 2006.

[13] H. K. Khalil, *Nonlinear Systems*, 3rd ed. Prentice Hall, 2002.

[14] T. I. Fossen, *Marine Control Systems: Guidance, Navigation and Control of Ships, Rigs and Underwater Vehicles*. Trondheim, Norway: Marine Cybernetics, 2002.

[15] P. Liljebäck, K. Y. Pettersen, and Ø. Stavdahl, "A snake robot with a contact force measurement system for obstacle-aided locomotion," in *Proc. IEEE Int. Conf. Robotics and Automation*, 2010, pp. 683–690.

[16] T. Lochmatter, P. Roduit, C. Cianci, N. Correll, J. Jacot, and A. Martinoli, "Swistrack - a flexible open source tracking software for multi-agent systems," in *IEEE/RSJ Int. Conf. Intelligent Robots and Systems*, 2008, pp. 4004–4010.

[17] P. Liljebäck, K. Y. Pettersen, Ø. Stavdahl, and J. T. Gravdahl, "Controllability analysis of planar snake robots influenced by viscous ground friction," in *Proc. IEEE/RSJ Int. Conf. Intelligent Robots and Systems*, 2009, pp. 3615–3622.

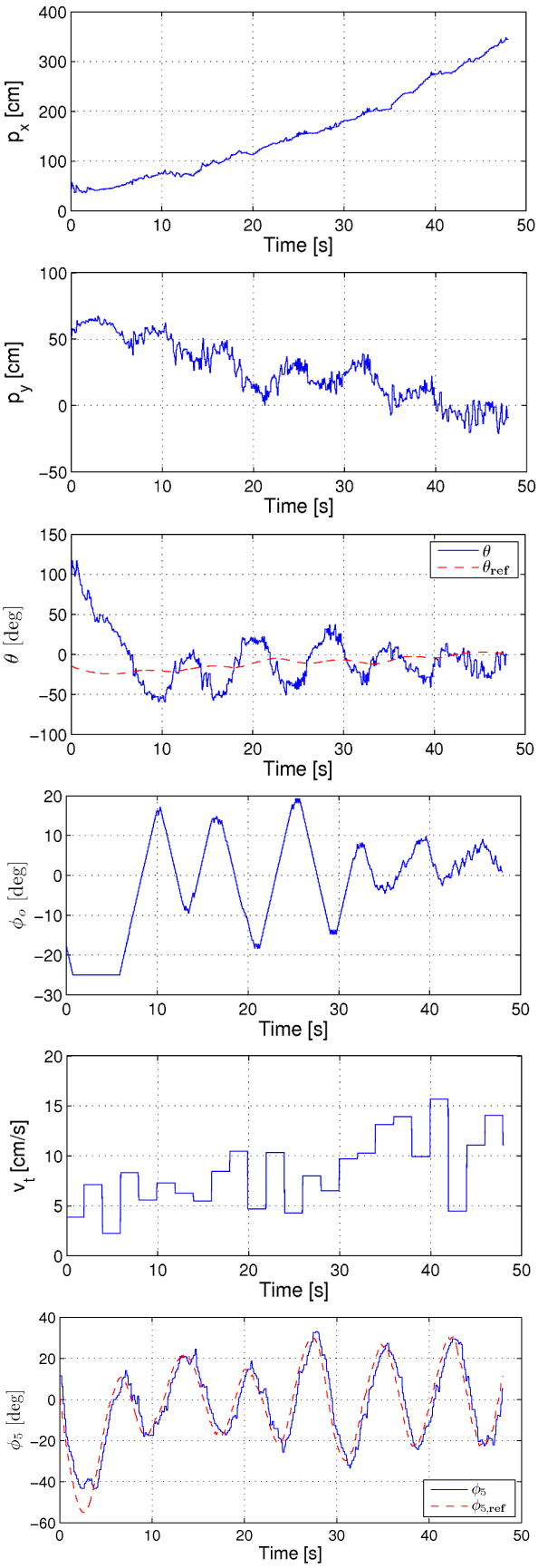

Fig. 10. The motion of the snake robot during path following with an initial heading away from the desired path.

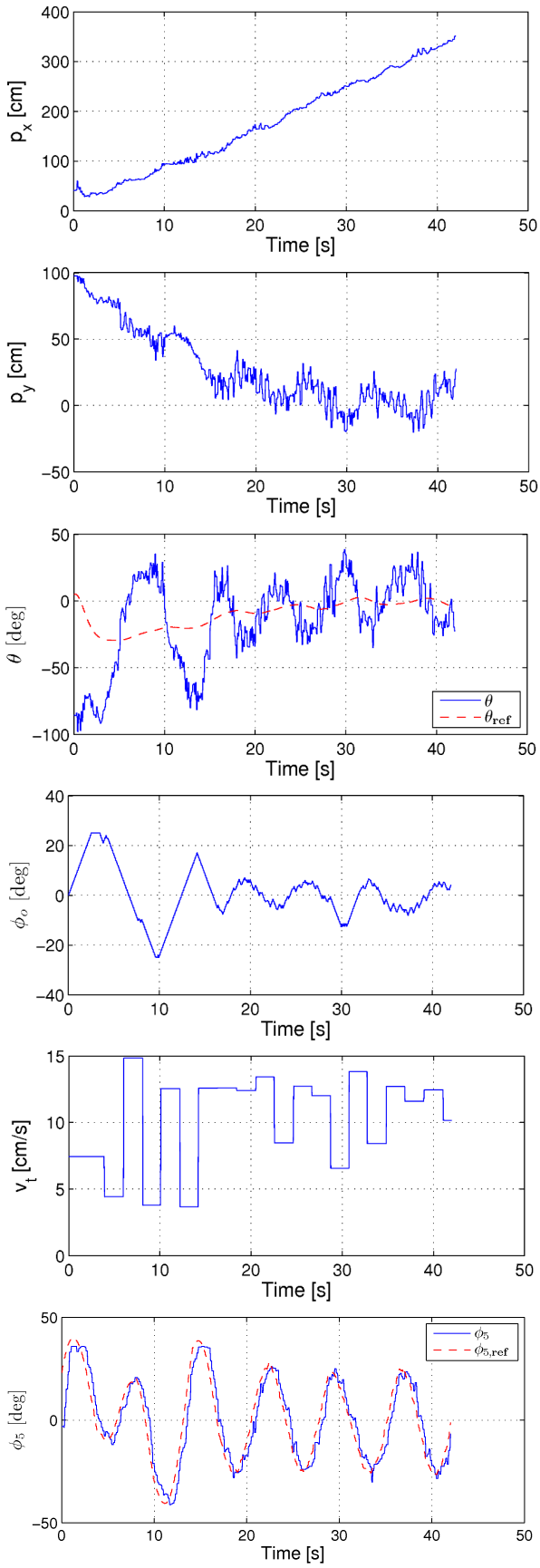

Fig. 11. The motion of the snake robot during path following with an initial heading towards the desired path.